RF CHARACTERISTICS OF P-WELL GaAs MESFETS[1]

Philip C. Canfield and David J. Allstot

Department of Electrical and Computer Engineering
Oregon State University
Corvallis, OR (503)737-3617

ABSTRACT

The first experimental results on the RF performance of p-well MESFETs are presented. It is shown that the small-signal equivalent circuit for the p-well MESFET must include a series RC branch between the source and drain to properly model the undepleted well and its contact. The dependence of the equivalent circuit parameter values on the doping of the p-well is presented and shown to have only a minor effect on the RF performance.

INTRODUCTION

The use of p-type implanted layers in n-channel GaAs MESFET technology is increasing due to the resultant improvements in key device characteristics. Previously reported improvements include smaller threshold voltage spreads (1), reduced short-channel effects (2), reduced frequency dispersion in the small-signal conductances (3), reduced drain current transients (4), and to some degree, improved backgating (5). The implant doses are generally chosen such that the p-layers are fully depleted under normal operating conditions. This insures maximum operating frequency, f_t, by minimizing the additional capacitance associated with the p-layers.

We have recently developed a GaAs p-well MESFET technology which uses an additional p^+ implant layer to contact the p-type region (p-well) which now completely surrounds the n-channel MESFET. A cross section of the p-well GaAs MESFET is shown in Fig. 1. By connecting this p-well contact to the n^+ source, the p-well is maintained at a fixed potential. As a result, the p-well MESFET technology totally eliminates backgating, drain current transients with long time constants, and frequency-dependence of the output conductance at low frequencies (< 100 kHz) (6). Thus, it is ideally suited for analog-digital IC applications. In this paper, we present experimental results on the RF performance of the p-well MESFET structure showing that it is also well-suited for microwave applications.

EXPERIMENTAL

The p-well MESFET's RF performance as a function of the p-well doping level, was evaluated using wafers fabricated with peak p-type implant concentrations of 2, 4, 8, and 16 x 10^{16} cm^{-3} below the n-type channel. A control wafer was also processed with no p-type implants. The n-channel implant doses of all wafers were adjusted so that all MESFETs had similar I_{dss} and V_p values. The S-parameters were measured using Cascade Microtech probes and an HP8510 network analyzer at frequencies between 100 MHz and 26.1 GHz at $I_{ds}=I_{dss}$ with $V_{ds}=2.5$ Volts. All measurements presented herein were taken from non-self-aligned recessed-gate devices with 300 um gate widths, 1 um gate lengths, and 3 um channel lengths.

EQUIVALENT CIRCUIT

The small-signal equivalent circuit model is derived directly from the physical structure of the p-well GaAs MESFET and is shown in Fig. 2. This model differs from more conventional models by the addition of a series RC branch between the drain and source. This branch accounts for the resistance of the undepleted portion of the p-type well connecting the p^+ contact to the source, and the depletion capacitance of the drain n^+-p-well junction. The equivalent-circuit model was implemented using Touchstone and the small-signal element values were optimized until the mean error between the measured and modeled S-parameters was less than 0.05 percent.

[1]This work has been supported in part by Tektronix, Inc. and was conducted in cooperation with TriQuint Semiconductor, Inc.

RESULTS

The modeled and measured S-parameters for a p-well device with the peak well doping of 16 x 10^{16} cm^{-3} are shown in Fig. 3. S_{11} and S_{22} are shown on the Smith chart in Fig. 3. Failure to include R_p and C_p in the model results in a poor fit as shown in Fig. 4. It is seen from Fig. 5 that the series RC network associated with the constrained p-well introduces a pole and zero (doublet) in the frequency response of S_{21}. For the wafers with lower p-type doping in the p-well, the magnitude of the shift is small due to the relative magnitude of R_p with respect to R_{ds} and therefore had much less effect.

The calculated equivalent circuit values of the capacitances, R_{ds}, R_p, and g_m for the equivalent circuit in Fig. 2 are shown in Figs. 6-12. The shifts in the values of C_{gs}, C_{gd}, and C_{ds} shown in Figs. 6-8 respectfully do not correlate with the doping of the p-type layers and are the result of variations in the threshold voltage from wafer to wafer. As expected, R_p decreases dramatically for the more conductive p-type layers as shown in Fig. 9, while C_p increases strongly as shown in Fig. 10. The dependence of R_{ds} on the p-well doping in Fig. 11 may be partially due to shortcomings of the optimization. From Fig. 5 it is seen that the pole-zero doublet introduced by R_p and C_p is at the lower boundary of the frequency spectrum for which data was measured. Thus the optimizer had to evaluate R_p, C_p, and to and to some extent R_{ds} from data available for only a couple of frequencies. The value of g_m is relatively insensitive to the p-type dose under the channel as shown in Fig. 12 and shows variations due to different threshold voltages of the different wafers. Fig. 13 shows that the transition frequency, f_t, changes only modestly, decreasing by less than 10 percent for the wafer with the highest p-type well doping as compared to the control wafer.

CONCLUSIONS

In this paper we have shown that the p-well GaAs MESFET is a viable device for microwave as well as precision analog-digital applications. An accurate small-signal equivalent-circuit model has been developed based on the physical structure of the p-well GaAs MESFET device.

REFERENCES

(1) Y. Umemoto, S. Takahashi, N. Matsunaga, and M. Nakamura, "GaAs MESFETs with a buried p-layer for large-scale integration," Electron. Lett., vol. 30, no. 2, pp. 98-100, Jan., 1984.

(2) K. Yamasaki, N. Kato, and M. Hirayama, "Buried p-layer SAINT for very high-speed GaAs LSI's with submicrometer gate length," IEEE Trans. Electron Dev., vol. ED-32, no. 11 , pp. 2420-2425, Nov., 1985.

(3) P.C. Canfield, D.J. Allstot, J. Medinger, L. Forbes, A.J. McCamant, B.A. Vetanen, B. Odekirk, E.P. Finchem, and K.R. Gleason, "Buried channel GaAs MESFETs with improved small-signal characteristics," IEEE GaAs IC Symposium Technical Digest, pp. 163-166, 1987.

(4) P. Canfield, L. Forbes, R. Gleason, and A. McCamant, "Drain current transient suppression in buried channel GaAs MESFETs," Proc. 4th Semi-Insulating III-V Materials Conf.: Hakone, H. Kukimoto and S. Miyazawa; eds., Tokyo: Ohmsha, LTD. and Amsterdam: North-Holland Publ. Co., pp. 573-578, 1986.

(5) E.P. Finchem, W.A. Vetanen, B. Odekirk, and P.C. Canfield, "Reduction of the backgating effect in GaAs MESFET ICs by charge trapping at the backgate electrode," IEEE GaAs IC Symposium Technical Digest, pp. 231-234, 1988.

(6) P.C. Canfield and D.J. Allstot, "A p-well GaAs MESFET technology," Digest of the IEEE Intern. Solid State Circuits Conf., Feb., 1990.

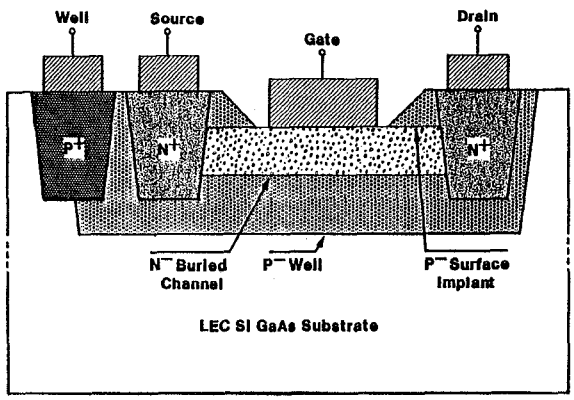

Fig. 1 Cross section of the p-well GaAs MESFET.

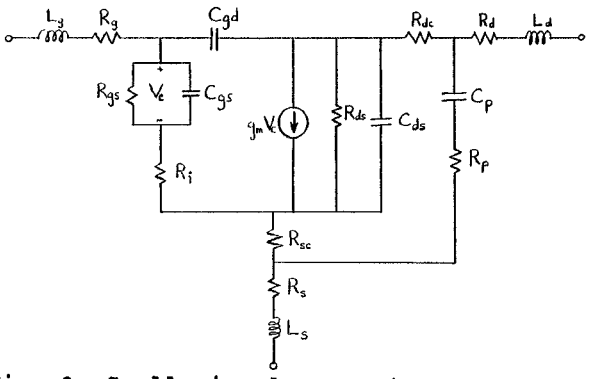

Fig. 2 Small-signal equivalent-circuit model used to model the p-well GaAs MESFET.

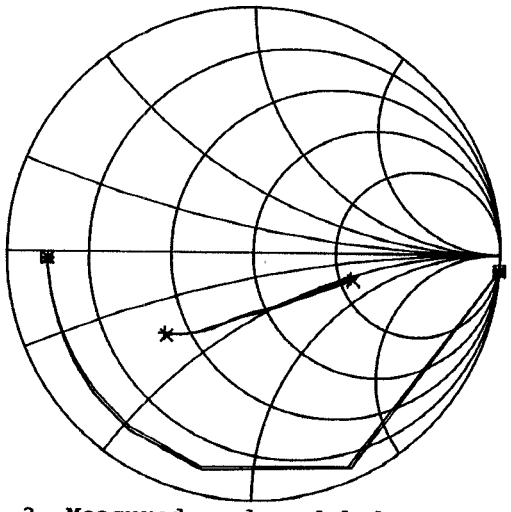

Fig. 3 Measured and modeled S_{11} and S_{22} for the model in Fig. 2. * measured S_{11}, = modeled S_{11}, X measured S_{22}, + modeled S_{22}.

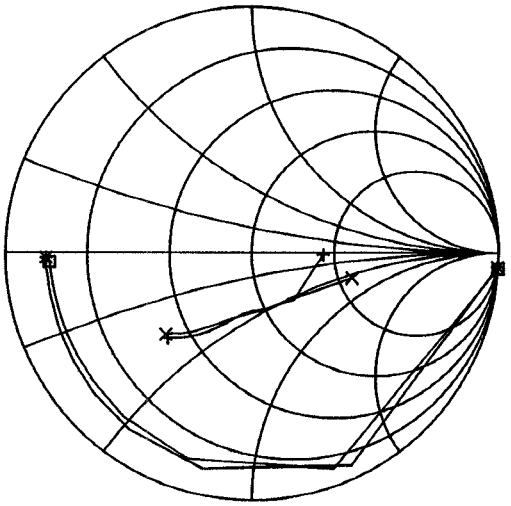

Fig. 4 Measured and modeled S11 and S22 for the model neglecting R_p and C_p. * measured S_{11}, = modeled S_{11}, X measured S_{22}, + modeled S_{22}.

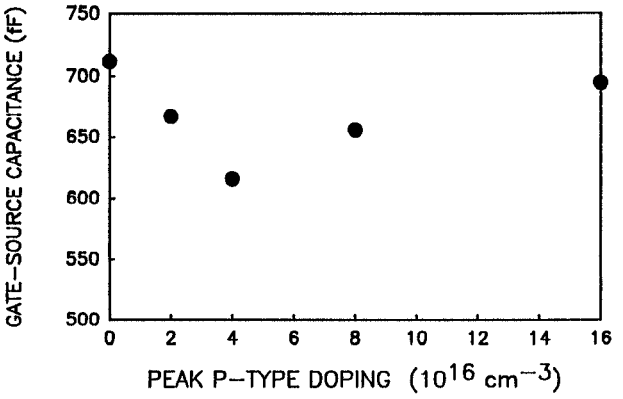

Fig. 5 Frequency response of S_{21} showing the pole zero doublet introduced by the series RC time constant.

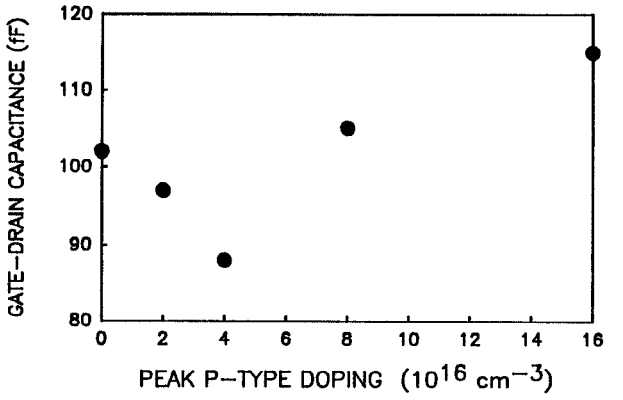

Fig. 6 Gate to source capacitance (C_{gs}) as a function of peak p-well doping.

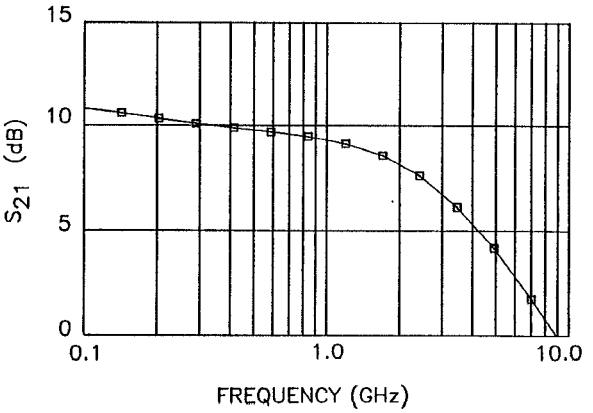

Fig. 7 Gate to drain capacitance (C_{gd}) as a function of peak p-well doping.

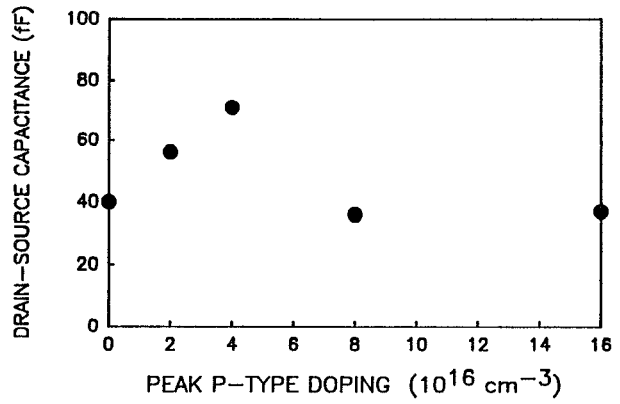

Fig. 8 Drain to source capacitance (C_{ds}) as a function of peak p-well doping.

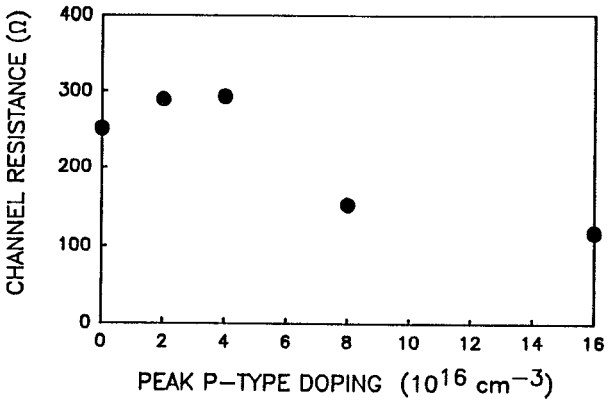

Fig. 11 Channel resistance (R_{ds}) as a function of peak p-well doping.

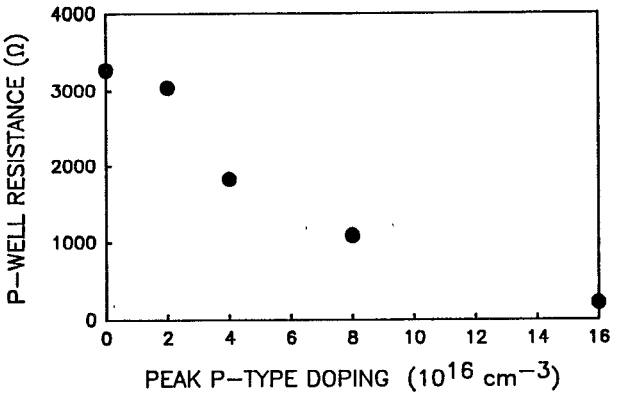

Fig. 9 Resistance associated with the undepleted p-region under the channel (R_p) as a function of peak p-well doping.

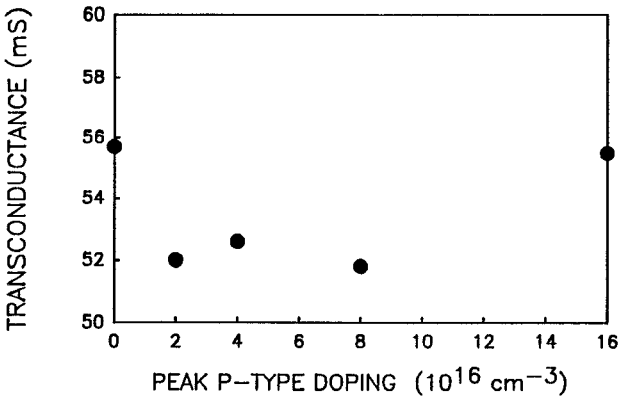

Fig. 12 Transconductance (g_m) as a function of peak p-well doping.

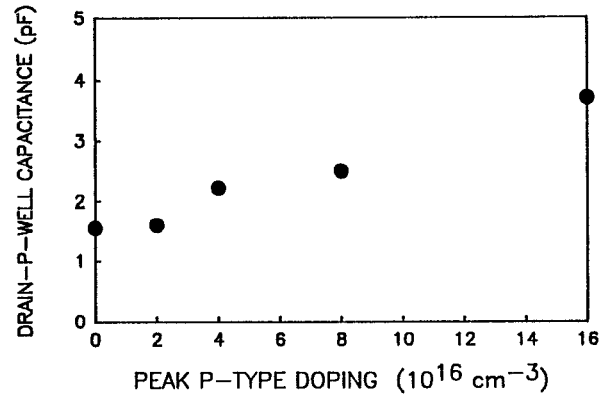

Fig. 10 Capacitance of depleted p-region near the drain (C_p) as a function of peak p-well doping.

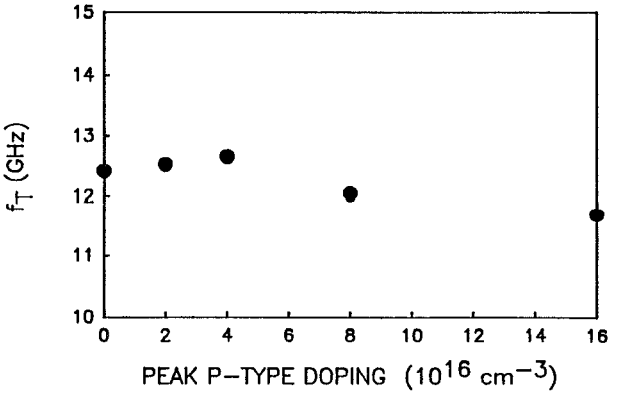

Fig. 13 Transition frequency (f_T) as a function of peak p-well doping.